Theoretical and Applied Fracture Mechanics 72 (2014) 76–88

Contents lists available at ScienceDirect

Theoretical and Applied Fracture Mechanics

journal homepage: www.elsevier.com/locate/tafmec

Multiscale modeling and prediction of bonded joint failure by using an adhesive process zone model

B. Ren, S. Li *

Department of Civil and Environmental Engineering, University of California, Berkeley, CA 94720, USA

ARTICLE INFO

Article history:
Available online 9 May 2014

Keywords:
Adhesive process zone model
Bonded-joint
Mixture failure mode
Cohesive zone model
Virtual internal bond

ABSTRACT

In this work, a three-dimensional multiscale adhesive process zone model (APZM) is used to simulate dynamic failure process of bonded joint structures. APZM combines the ideas of the cohesive zone model (CZM), the Cauchy–Born rule, and the so-called virtual internal bond (VIB) theory to predict failures of bonded joints that involves adhesive failure, cohesive failure, and mixture of both. The proposed APZM has some unique advantages to describe mechanical behaviors of bonded joints under general loading conditions. First, in contrast to conventional FEM model, APZM model can simulate dynamic fracture process of structure without remeshing. Second, APZM replaces the ad-hoc traction–separation laws of interface used in CZM with full three-dimensional interphase model, which is based on the VIB theory. Consequently, APZM can naturally capture both mixed failure modes as well as mixture failure mode under complex loading conditions. Third, an empirical elastic energy density function for macromolecular polymers was constructed, and its material parameters are obtained by calibrating the model with material properties measured from experiments such as under pure tension and shear tests. In order to validate APZM model and to predict stress field in adhesive layer accurately, a series of numerical simulations of bonded joints under shear, tension and mixed loading conditions have been conducted. The numerical results indicate that APZM can accurately predict the failure modes as well as the dynamics fracture process of bonded joints.

1. Introduction

In comparison with fastened joints that suffer from the stress concentration and material damage near fasteners, the adhesively bonded joints, which transfer energy and moment through the adjacent adherend to the adhesive layer, are extensively used in aero crafts, watercrafts, and automobile structures. Despite the advantages associated with the bonded joint, the adhesives used to bond the metals or composites are usually less resistant to mechanical loading and chemical actions, they are also more susceptible to aging than mechanical fastenings. In engineering practice, these joints are probably the weakest links in the whole structure. A great deal of research effort has been made over the past decades on developing modeling and simulation tools on the adhesively bonded joints [1]. Due to its specific configuration and complex interaction between adhesive layer and adherends, there are still some challenging technical issues to be resolved in order to accurately predict the failures of bonded joint structures.

To compute the stress field along joint surface, early attempts were devoted to find close-form solutions of joints under various loading conditions. The most notable models were developed by Volkersen [2], and Goland and Reissner [3]. Both of these models simplify the stress field in adhesive layer as plane stress state. More generally, Crocombe and Bigwood [4] modified the plane stress mode to include the out-plane normal stress and anti-plane shear stress. With the development of finite element method, recent stress analyses of bonded joints have employed both 2D and 3D finite element methods [5,6]. The numerical results obtained by FEM analyses can capture more realistic stress fields, which reveal that traditional analytical approaches are inadequate [6]. However, there are several issues in FEM analyses of bonded joints: First FEM analyses are heavily relied on the material constitutive models used for adhesives. Traditionally, the adhesives are treated either as linear-elastic solids [6], or nonlinear elastic solids, or even elastic–plastic solids at macro-scale [7]. Such modeling technique is fundamentally flawed. This is because that the adhesive materials are macromolecular compounds, and their underlying structures are essentially long, randomly oriented, and cross-linked molecular chains network that are basically

* Corresponding author. Tel.: +1 5106425362; fax: +1 5106438928.
E-mail address: shaofan@berkeley.edu (S. Li).

http://dx.doi.org/10.1016/j.tafmec.2014.04.007
0167-8442/

viscoelastic or visco-elastoplastic polymers at macroscale. Moreover, they usually undergo large nonlinear elastic deformations during work load. Second, conventional FEM model cannot simulate fracture with strong discontinuities without remeshing. Many researches have investigated the adhesive material responses at microscale or mesoscale. Bergström and Boyce [8] constructed a two-body interaction potential for the rubber-like polymer, and they studied the material properties based on its chemical molecular structure at molecular scale.

Another important technical challenge is how to model the failure process in computer simulation. The experimental tests and engineering practices revealed that there are three essential failure modes along the bonded surface associated with different loading conditions [9]: (I) cohesive failure, i.e. the crack penetrates inside the adhesive layer; (II) adhesive failure, i.e. the failure occurs along the interface between adherends and adhesive; and (III) the mixture of both cohesive and adhesive failures. In the case of composite adherends, an additional first ply failure mode may occur for specific type of joints [10]. Note that there is a difference between the mixture failure mode and the mixed fracture mode. In the bonded joints failure analysis, the mixture failure mode is referred to the failure mode involving both adhesive as well as cohesive failures, which may occur during mixed-mode loadings. However, it may also be possible during pure tension or pure shear loadings, and it is in fact an open question in the bonded joint failure analysis. For the composite double lap bonded joints, the primary failure mode is the cohesive failure in the first ply of the parent laminate, and less dominant failure modes are cohesive failure in the adhesive layer, as well as adhesive failure between the adhesive layer and the first ply. To determine the onset of failures, some failure criteria have been suggested in the literature, such as the critical strain energy by Ratwani et al. [11]. Ignjatovic et al. [12] proposed the static and residual strength models, in which the damage process is triggered when the strain energy G in bonded joint reaches a critical value G_c. The specific value of G_c for given bonded joint is obtained by the experimental test or measurement. Hart-Smith [10] predicted the strength of bonded joints using a failure criterion based on the critical value of the first invariant of strain tensor. It was shown that the predicted bonded joint strength agreed well with the experimental data. More recently, the cohesive zone model (CMZ) has become popular in numerical simulation of bonded joint failures. This is because that the thin adhesive layer in bonded joints can be modeled as a cohesive surface [13,14]. The CZM approach to bonded joint analysis basically considers the bonded joint failure as an interlaminar fracture, rather than bulk material failure or intra-laminar failure; and the bonded joint strength is described by the prescribed cohesive law that does not distinguish the cohesive failure mode or adhesive failure mode specific to the bonded joint structures. In general, the CZM-based failure criterion can accurately reflect the physical nature of interlaminar failure of adhesive layer or the composite adherends. The additional advantage of CMZ approach is that CMZ is a proven successful approach predicting failure of interface fracture. However, the conventional CMZ is based on ad-hoc traction–separation laws that are obtained from the experiments of Mode I, II, and III loadings separately. As mentioned above, a bonded joint structure is usually under general mixed-mode loading conditions, which does not conform to any of those failure loading modes. Moreover, the traditional cohesive-zone model considers the adhesive layer as zero thickness, thus CZM approach cannot predict adhesive failure, as well as the mixture failure mode that involves both cohesive and adhesive failures. Extending the theory of CZM, Zeng and Li [19], Li et al. [20] and Ren and Li [15] proposed an atomistic-based process zone model (APZM) to simulate fracture and fragmentation of polycrystalline solids at mesoscale, which considers the material interphase, such as grain boundary or persistent slip bands, as a finite thickness zone, and they have calculated the stress field in crystalline solids by using the Cauchy–Born rule based atomistic-enriched continuum theory.

In this work, we propose and apply a novel adhesive process zone model (APZM) to simulate dynamic stress field inside the adhesive layer, and subsequently to predict the failure of adhesive bonded joints. We have shown that the proposed APZM tool can be used in analysis of bonded joints, including structure and material designs, stress and failure analysis, non-destructive detection analysis, and reliability analysis. The central idea of this approach is to replace the ad-hoc interface traction–separation law in CZM with a 3D constitutive model that is derived from an adhesive energy

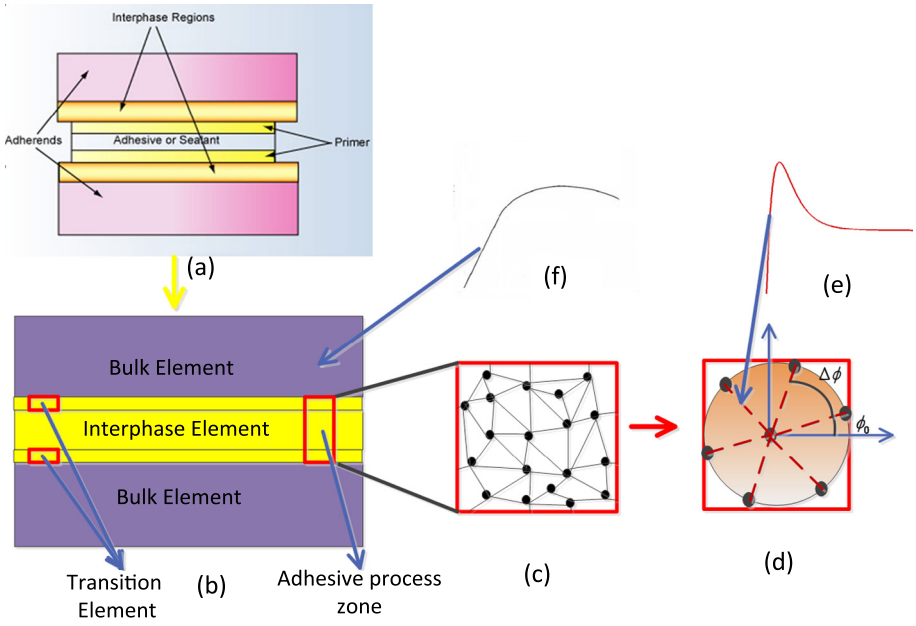

Fig. 1. The schematic illustration of adhesive process zone model. (a) The actual structure of bonded joint; (b) the adhesive process zone model with transition zone and interphase zone; (c) the material network of adhesive process zone with random virtual internal bonds; (d) the representative unit cell with representative lattice of adhesive process zone; (e) the adhesive constitutive law; and (f) classical elasto-plastic constitutive law of adherend.

function that is calibrated with the experimental tests under both tension and shear loadings. A major difference between APZM and CZM is that APZM considers the adhesive layer as a three dimensional solid material. In doing so, every components of stress field are calculated by using the virtual internal bond theory (VIB). Consequently, both adhesive failure, cohesive failure, as well as the mixture failure modes in bonded joints with different geometric configurations or under complex loadings can be captured.

This paper is organized as follows: in Section 2, we describe the Cauchy–Born rule based continuum theory and the VIB theory; Section 3 focuses on the proposed APZM and how it is applied to analyze bonded joints; in Section 4, we discuss the proposed empirical adhesive energy function, and its calibration of the open parameters with experiments; in Section 5, we discuss the finite element formulations of APZM as well as their computer implementation; in Section 6, a series of numerical simulations are reported, and their results are compared with experimental test date. Finally to close the presentation, a few remarks are made in Section 7.

2. Cauchy–Born rule based continuum theory

As a macromolecular material, the adhesives inside the bonded joint consist of long, cross-linked, and randomly oriented molecular chains at microscale or mesoscale [8]. This essential molecular structure leads to non-linear elastic responses at macro-scale. To model polymer material more accurately, one has to take into account its molecular origin. Therefore, we adopt the Cauchy–Born rule to relate the motion of micro-scale molecules or atoms with the continuum deformation measured at macro-scale [15]. The so-called Cauchy–Born rule assumes that in a local region at micro-scale, which may be viewed as a point at macro-scale, when the deformation is uniform or homogeneous, the deformed material position vector can be expressed by its undeformed counterpart as $\mathbf{r} = \mathbf{F} \cdot \mathbf{R}$, where $\mathbf{r}$ is the deformed material position vector, $\mathbf{R}$ is the undeformed material position vector, and $\mathbf{F}$ is the deformation gradient tensor. Since the local deformation is uniform, the deformation gradient $\mathbf{F}$ is a constant tensor in this case. At micro-scale, each atom is surrounded by its neighboring atoms; the interaction force between two atoms is called the bond force, which mainly depends on the bond distance between the two atoms. For crystalline materials, the neighboring atom distributions have specific patterns that are called the lattice, and

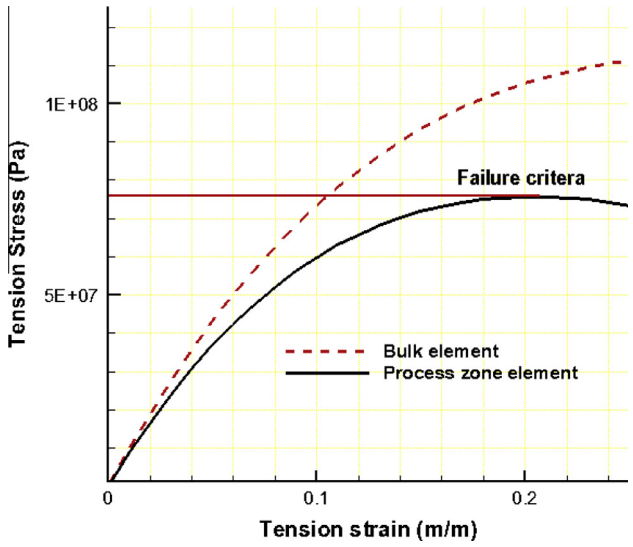

Fig. 2. Stress–strain relation and failure criterion inside process zone element.

Table 1
The parameters for adhesive FM-73.

Parameter	Value	Unit
D_0	7.43137e5	J
C	14.7	none
r_0	1.0	mm
β	0.5	none

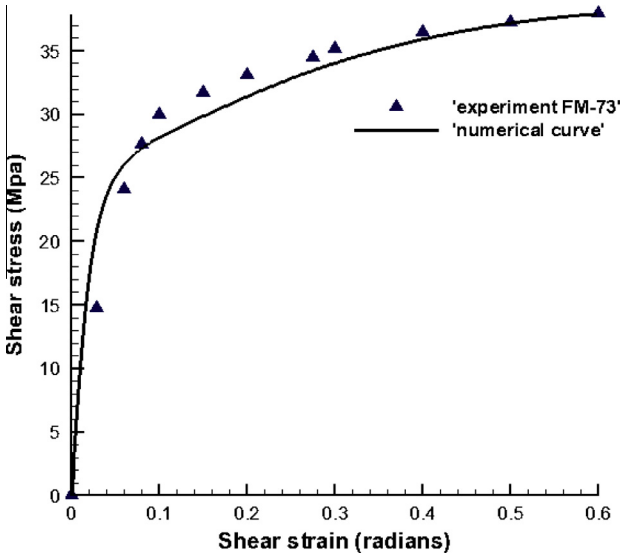

Fig. 3. The APZM and experimental shear stress–strain relations for FM73 adhesive.

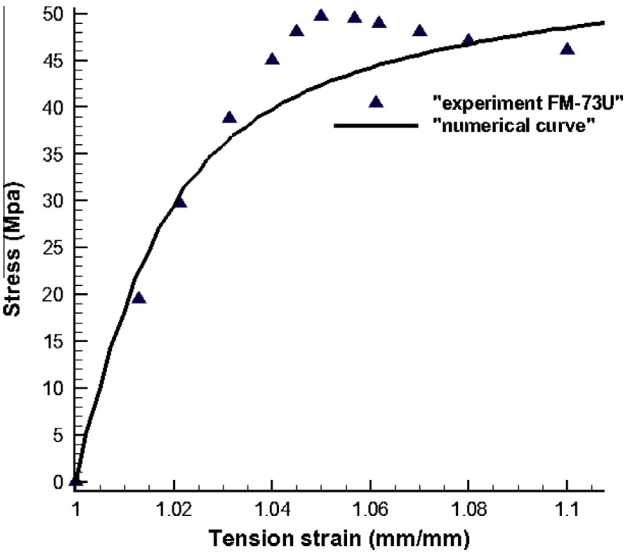

Fig. 4. The APZM and experimental tension stress–strain relations for FM73U adhesive.

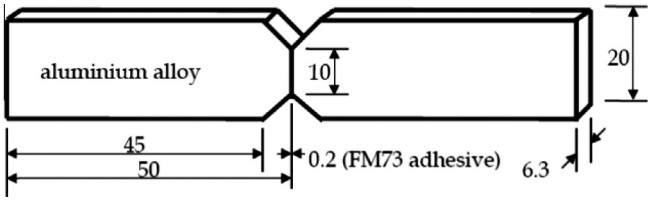

Fig. 5. Specimen dimensions in mm.

FCC, BCC, HCP lattices are most common lattice types for metallic and ceramic materials. In this case, the material position vector used in the Cauchy–Born rule may be understood as the lattice vector.

Assume that each of deformed bond has a stored potential energy, $E(\boldsymbol{r}_i)$, which is a function of the bond length. We can then use the Cauchy–Born rule to extrapolate the macroscopic strain energy $W(\boldsymbol{F})$ at each material point from the interatomic potential energy of that material, i.e.,

$$W(\boldsymbol{F}) = \sum_{i=1}^{n} E_a(\boldsymbol{r}_i) \tag{1}$$

Because the Cauchy–Born rule bridges the atomic scale and the continuum scale, we often call it a multiscale method. Gao and Ji [16] extended the concept of Cauchy–Born rule to a general class of amorphous materials to form a so-called virtual internal bond (VIB) theory. The VIB theory can be used to model the polymer as a homogeneous hyperelastic solid with a network of internal cohesive bonds, which is not necessary at atomic level. Consequently, the VIB model defines that the strain energy $W(\boldsymbol{F})$ of a given material point equals the elastic energy potential of all virtual internal bonds attached to that point:

$$W(\boldsymbol{F}) = \sum_{i=1}^{n} E(\boldsymbol{r}_i) \tag{2}$$

Thus we can apply VIB theory to describe the material properties of adhesive material in terms of intermolecular bond among macromolecule polymers. At meseoscale, macromolecular polymer chains may also be regarded as "bonds".

Although their cross-link formation might seem to be random, they also form a network similar to a "lattice" in crystalline solids. This cross linked network is not at atomistic scale, and the interaction among the macro-molecules is the intermolecular force. In engineering simulations, both triangle and tetrahedron lattice structures have been used to simulate the polymer materials with cross linked polymer chain micro-structure, e.g. [23,24]. In this work, we employ a spatial tetrahedron lattice structure to model the cross linked chain network micro-structure that commonly present in the adhesive materials inside the bonded joints. This "lattice" structure resembles the FCC structure, and for each molecule particle or cluster it has 12 virtual bonds connecting to it, and they are located at the position,

$$\mathbf{R}_i : \left(\pm\frac{\sqrt{2}}{2}R_0, \quad \pm\frac{\sqrt{2}}{2}R_0, \quad 0 \right) i = 1,2,3,4$$

$$\mathbf{R}_i : \left(\pm\frac{\sqrt{2}}{2}R_0, \quad 0, \quad \pm\frac{\sqrt{2}}{2}R_0 \right) i = 5,6,7,8$$

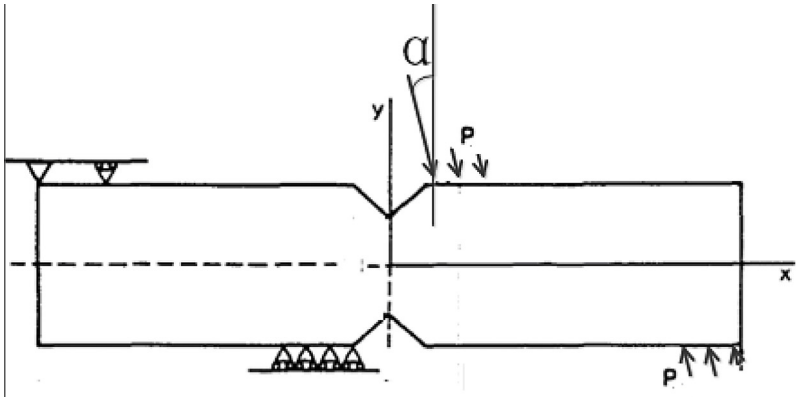

(a) The boundary condition

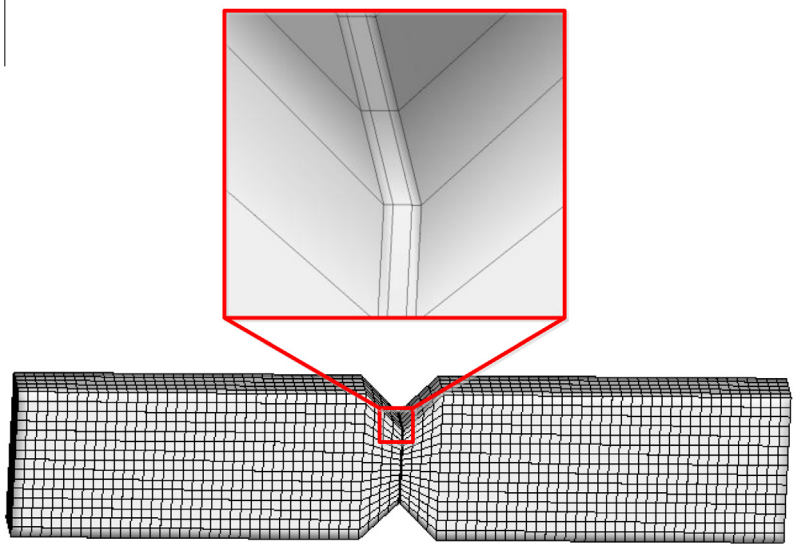

(b) The computational mesh

Fig. 6. The finite element mesh.

$$\mathbf{R}_i : \left(0, \quad \pm\frac{\sqrt{2}}{2}R_0, \quad \pm\frac{\sqrt{2}}{2}R_0\right) i = 9, 10, 11, 12$$

$$R_0 = |\mathbf{R}_i| \tag{3}$$

if the molecular cluster interested is located at the origin of the local coordinate, i.e. (0,0,0). Here R_0 is the equilibrium bond length, which is exactly the same as that in molecular dynamics (MD) simulation. Associated with deformation gradient **F**, the deformed virtual internal bonds are calculated as:

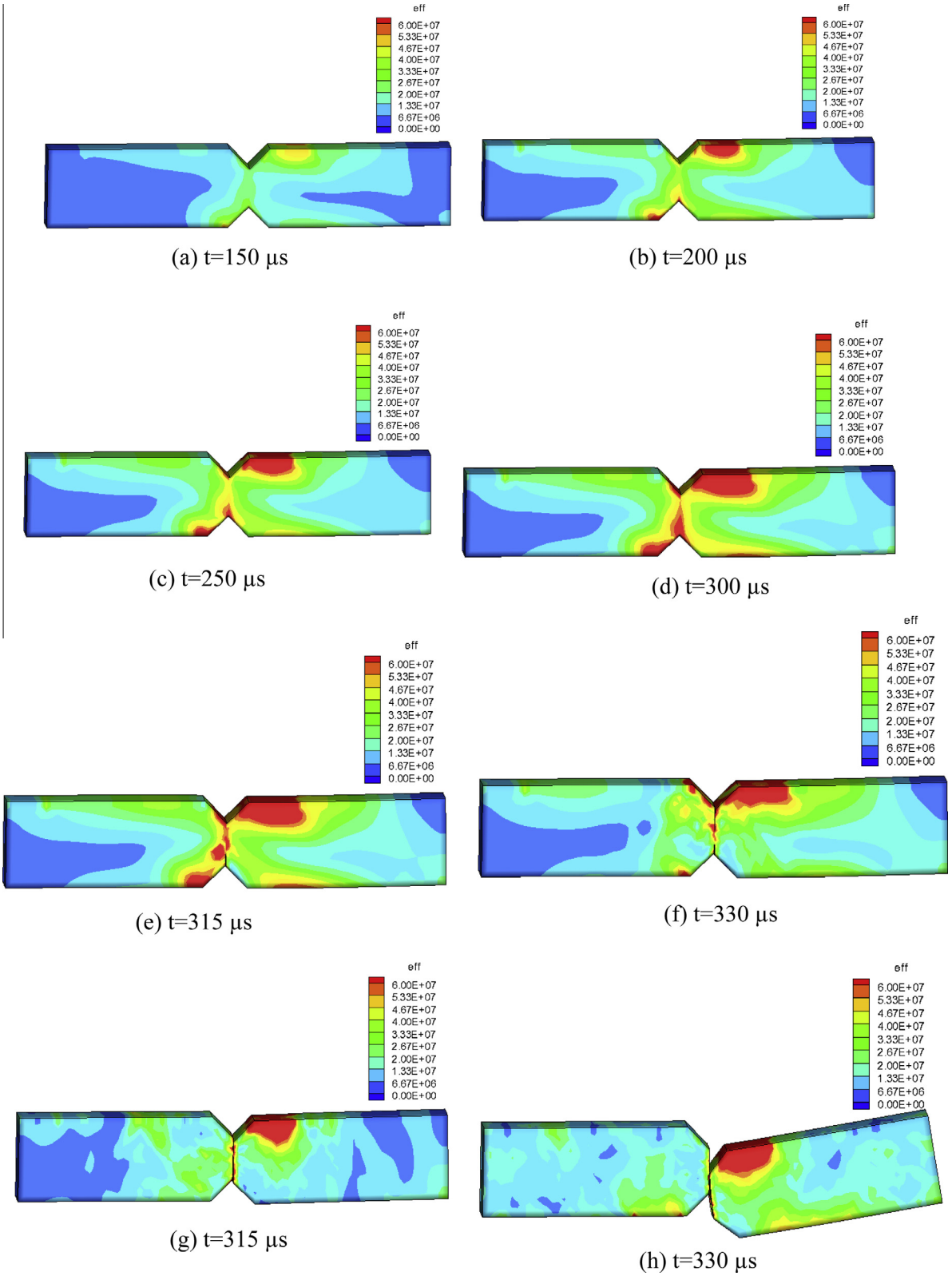

Fig. 7. The time sequences of failure process under pure shear loading (effective stress).

$$\mathbf{r}_i = \mathbf{F}\mathbf{R}_i \quad i = 1, 2 \ldots n \tag{4}$$

with bond length $r_i = |\mathbf{r}_i|$.

Consequently, we can derive the hyperelastic constitutive relation from energy density function:

$$\mathbf{S} = 2\frac{1}{\Omega_0}\frac{\partial W(\boldsymbol{F})}{\partial \mathbf{C}} = \frac{1}{\Omega_0}\sum_{i=1}^{n}\frac{\partial E(\boldsymbol{r}_i)}{\partial r_i}\frac{\partial r_i}{\partial \mathbf{C}} = \frac{1}{\Omega_0}\sum_{i=1}^{n}\frac{\partial E(\boldsymbol{r}_i)}{\partial r_i}\frac{\mathbf{R}_i \otimes \mathbf{R}_i}{r_i} \tag{5}$$

where $\mathbf{S}$ is the 2nd Piola Kirchhoff stress (PK_II stress). $\mathbf{C} = \mathbf{F}^T\mathbf{F}$ is the right Green Deformation tensor. Ω_0 denotes the volume of a unit cell.

Although using the symmetric 2nd Piola–Kirchhoff stress is more convenient in the constitutive modeling, it may result a cumbersome expression in the equation of motion. Alternatively, we use the 1st Piola–Kirchhoff stress $\mathbf{P}$ to establish the Galerkin weak formulation in finite element analysis,

$$\mathbf{P} = \mathbf{F}\mathbf{S} = \frac{1}{\Omega_0}\sum_{i=1}^{n}\frac{\partial E(\boldsymbol{r}_i)}{\partial r_i}\frac{\mathbf{R}_i \otimes \mathbf{r}_i}{r_i} \tag{6}$$

By doing so, we can use the VIB theory to bridge the molecular theory of the adhesive energy function with the continuum theory of stress analysis under finite deformation.

3. The adhesive process zone model in bonded joints

To fundamentally solve bonded joint analysis problem, the proposed adhesive process zone model (APZM) (Fig. 1) combines the virtual internal bond theory (VIB) [16] with an interphase model. The basic idea of APZM is to replace the zero-thickness cohesive surface in CZM with the finite thickness adhesive process zone where the constitutive relation is constructed by VIB theory from certain adhesive energy potential. In principle, the proposed technology is superior to CZM based interface adhesive analysis as well as the traditional stress-based FE analysis in regards to its physical modeling fidelity, numerical computation accuracy, engineering reliability, and experimental validation.

The actual geometric configurations of bonded joints are diverse, and sometimes they can be very complex, e.g. [1,5–7]. However, in principle, a representative geometric configuration of the bonded joint can always be treated as two adjacent adherend plates sandwiching a very thin adhesive layer as shown in Fig. 1(a). In this work, the thin adhesive layer is modeled by the proposed adhesive process zone model (APZM).

Employing FEM discretization, two adherends of the bonded joint will be discretized by conventional 3D finite elements, such as brick elements or tetrahedron elements, which we refer as bulk elements. The failure modes of bonded joints depend on loading conditions, and it could be cohesive failure, adhesive failure or mixture of cohesive and adhesive failure. To predict and capture the correct failure mode under given loading condition, the adhesive process zone will be subdivided as three sub-layers, in which the middle layer of interphase zone is sandwiched by two layers of transition zones. The transition zone and interphase zone are discretized by using conventional 3D finite elements the same as the adherends, except that they have extreme small thickness or very large dimensional aspect ratio. The transition elements share nodes with both bulk elements and interphase elements (Fig. 1(b)). The entire bonded joint structure are discretized as finite element mesh eventually, however the element sizes in different regions are drastically different. The adhesive process zone with finite thickness ($\sim 10^{-4}$ m) can be considered as a homogeneous, isotropic solid with a microstructure consisting of internal adhesive bonds between a randomly distributed particles as shown in Fig. 1(c); here the particles are molecule cluster, which are not necessary atoms. The distribution of particles forms a continuous field

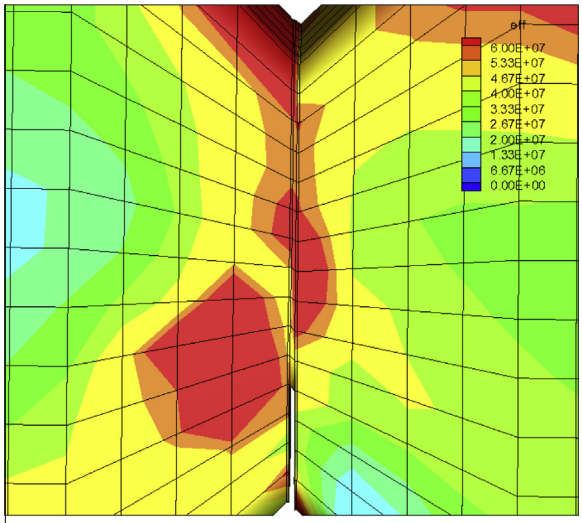

(a) t=315 μs

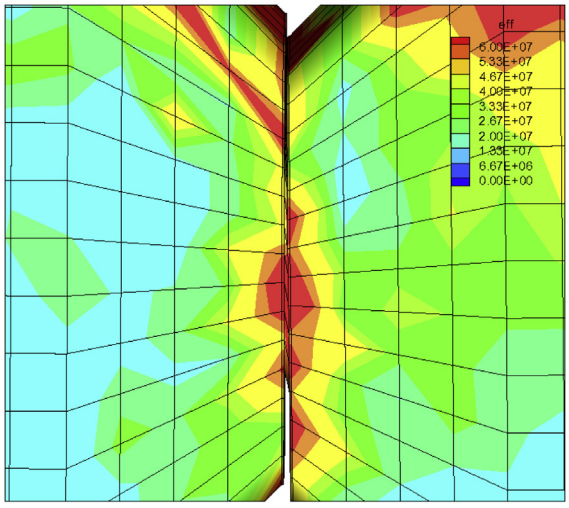

(b) t=335 μs

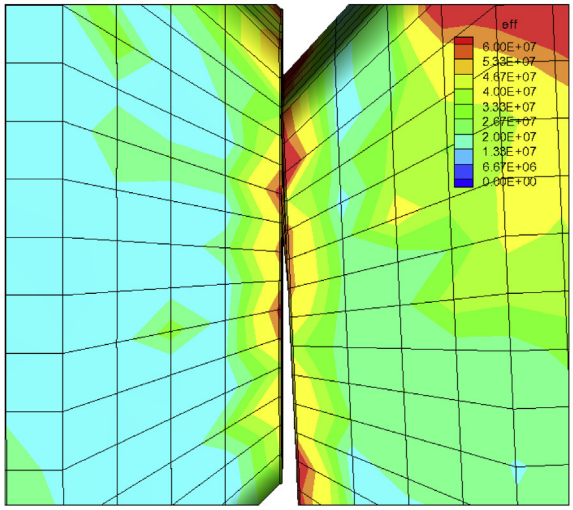

(c) t=365 μs

Fig. 8. The dynamic process of cohesive failure.

that is described by the quasi-continue VIB theory, and its physical behaviors can be represented by certain representative unit cell

Table 2
The comparison of numerical and experimental results.

Loading model	Loading angle (α, degree)	Adhesive thickness (mm)	Failure mode (experiment)	Failure mode (numerical)	Failure loading (experiment) (kN)	Failure loading (numerical) (kN)
Pure shear	90	0.2	Cohesive failure	Cohesive failure	2.38	2.36
Pure tension		0.20	Adhesive failure	Adhesive failure	2.40	2.75
Shear and compression	17.19	0.20	Mixture of adhesive and cohesive	Mixture of adhesive and cohesive	2.6	2.2

with finite virtual internal bonds, i.e., lattice, shown as Fig. 1(d). The mechanical response of this network is governed by certain adhesive constitutive relations as shown in Fig. 1(e). On the other hand, the mechanical response of adherend materials are simply treated as a continuum solid shown Fig. 1(f). However, sometimes we adopt special constitutive modeling for adherend such that it failure criterion is embedded into the bulk constitutive relation, for instance using the VIP theory based constitutive model.

In APZM, the kinematic field (displacement) of the whole structure is modeled as regular FEM approximation through element interpolation functions.

The initial process zone elements, i.e. transit elements and interphase elements (Ω_0), will deform into its current shape (Ω_t) at time t with specific deformation gradient ($\mathbf{F}$) at each element that can be calculated by the finite element method. This deformation leads to the change of strain energy density, and then it results the change of stress state in adhesive process zone as Eq. (5). This stress works as 'glue' to resist the separation of adjacent bulk elements (remember that the transit element and bulk elements share nodes along the adhesive surface). Normally the strength of adhesive is lower than that of adherend material. Once the stress state of adhesive reaches its peak value, such as the horizontal line in Fig. 2, the process zone elements become unstable. It will result fracture that separates it from the adjacent bulk elements. Fig. 2 illustrates the stress–strain relation and failure criterion inside the adhesive process zone element under the condition of pure tension.

Because in both bulk elements and process zone elements the full stress components are being evaluated, APZM can capture the mixed fracture mode naturally. In the case of lower bulk strength, one can set a few layers of bulk elements as process zone elements to allow crack reaching and penetrating to the adherends.

In APZM, there is no presumed fracture criterion for crack initiation, or there is no need to have a fracture criterion as FEM calculation because the failure criterion is embedded in the relation of constitutive laws of adherends and adhesive (Fig. 2).

Moreover, in contrast with conventional FEM or X-FEM, which need an artificial mesh updating algorithm to represent growing crack surfaces, such as level set method [21,22], the APZM can simulate interphase failure through the automatic annihilation of adhesive process zone elements just like the annihilation of the interface elements of CZM.

4. Calibration of APZM with experimental data

In APZM, the mechanical response of adhesive process zone material is derived from the adhesive energy function by using VIB theory as shown in Eq. (5). In this particular procedure, a crucial step is how to construct the adhesive potential energy function, $E(\boldsymbol{r}_i)$, that can accurately represent the non-linear elastic behavior of specific adhesive. There have been many literatures discussing atomistic potential functions for polymers [8] as well as polymeric composite [23]. Nevertheless, those atomistic potentials are intended for molecular simulations at microscale, whereas APZM computes the stress from adhesive potential energy function at macro-scale level. The macro-scale mechanical responses of engineering materials are much different with that in micro-scale. Therefore, in this work we do not directly construct the adhesive potential energy function from the atomistic potential. Instead, by referring some features of atomistic potential of adhesive [8], an empirical adhesive energy function is adopted for the adhesive constitutive relation, which can be expressed as,

$$E(\boldsymbol{r}_i) = D_0\left(-L(B)\beta_i - ln\left(\frac{\sinh(\beta_i + B)}{\beta_i + B}\right)\right)\Big/C \tag{7}$$

$$\beta_i = C^2(r_i - r_0)/r_0 \tag{8}$$

where L is a Langevin function that is defined as follow

$$L(\beta_i) = \coth(\beta_i) - \frac{1}{\beta_i} \tag{9}$$

In Eq. (8), r_i is the current bond length of i-th virtual bond, r_0 is the bond length at equilibrium position as that in atomistic potential.

Then the derivative of adhesive energy function $\frac{\partial E(\boldsymbol{r}_i)}{\partial r_i}$ used in Eq. (5) can be written as,

$$\frac{\partial E(\boldsymbol{r}_i)}{\partial r_i} = D_0 C(-L(B) + L(\beta_i + B))/r_0 \tag{10}$$

In Eq. (10), there are 4 open parameters that define specific adhesive material: D_0, B, C, r_0. In this paper, the adhesive material is set as FM-73 adhesive, whose experimental stress–strain relation under tension and shear loading can be found in the literature, e.g. [17,18]. We can determine the values of open parameters as shown in Table 1 by fitting the adhesive constitutive relations with

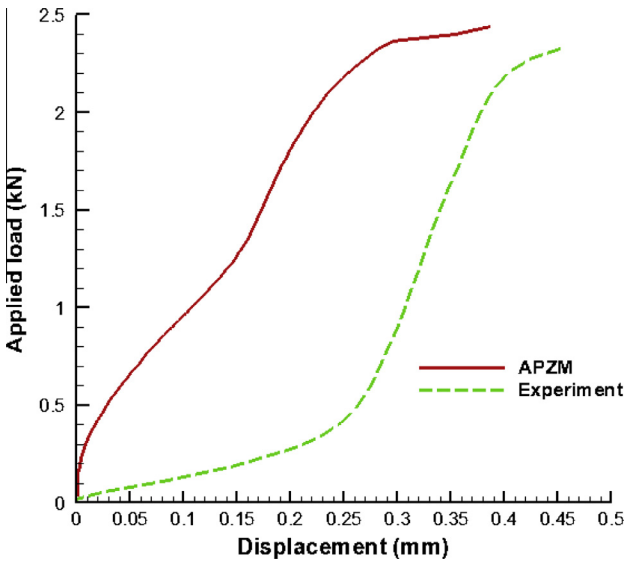

Fig. 9. The loading–deflection curves under pure shear.

experimental date as shown in Figs. 3 and 4. Note that the material used in the tension experiment is the adhesive FM-73U, which may have some difference with the material used in the shear test, which is the adhesive FM-73.

The adhesive constitutive relations displayed in Figs. 3 and 4 show that the adhesive will become unstable when it reaches the yielding phase. In computations, we set up a failure criterion for each molecular virtual bond: when the bond length satisfies the condition: $r_i \geqslant 1.33r_0$, then the bond will break. This criterion is not set arbitrarily. This critical bond value is selected, because the simulation results obtained under such criterion fit best with experimental data (Fig. 3). In particular, it can

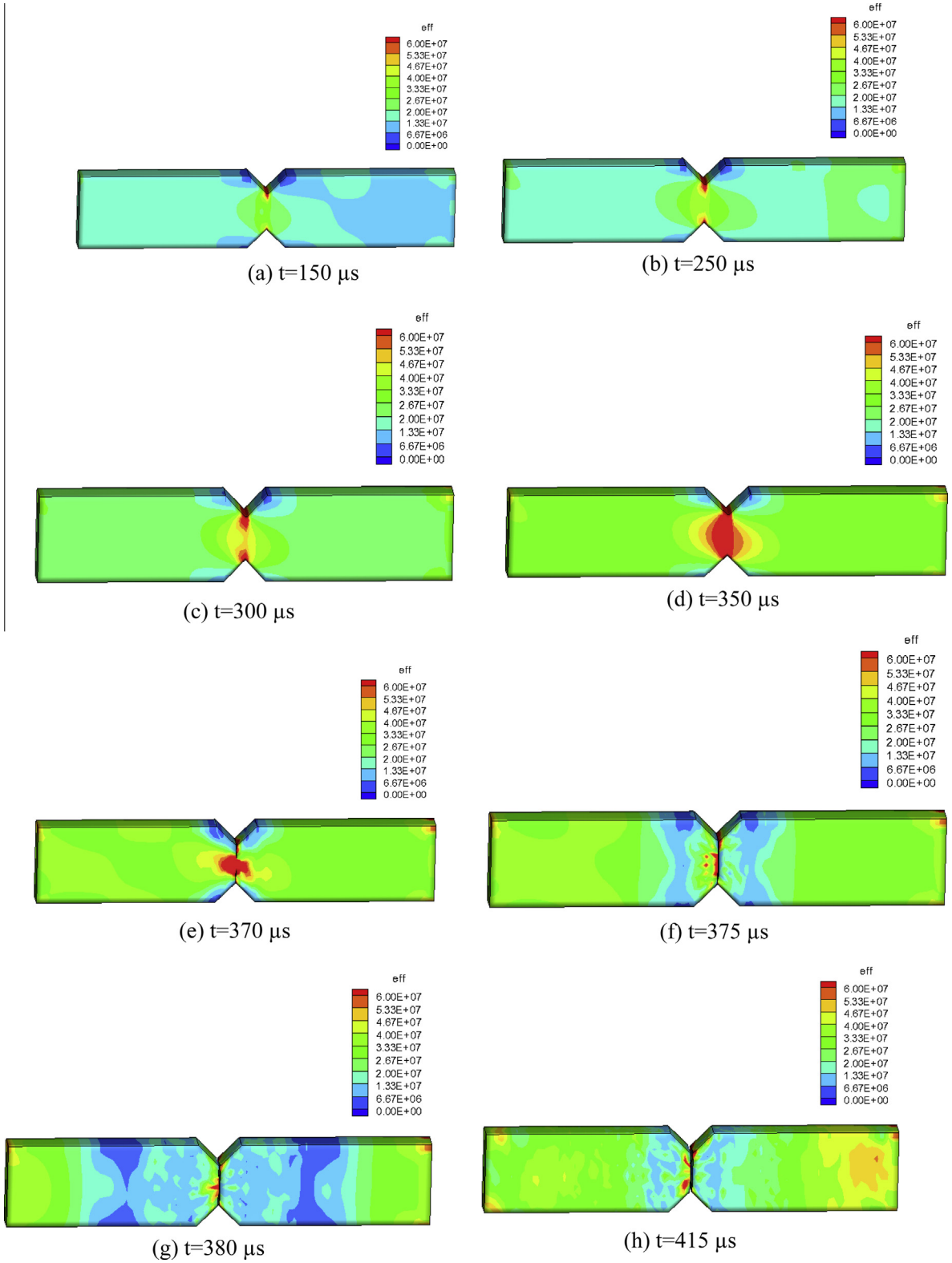

Fig. 10. Time sequences of failure process under pure tension loading (effective stress).

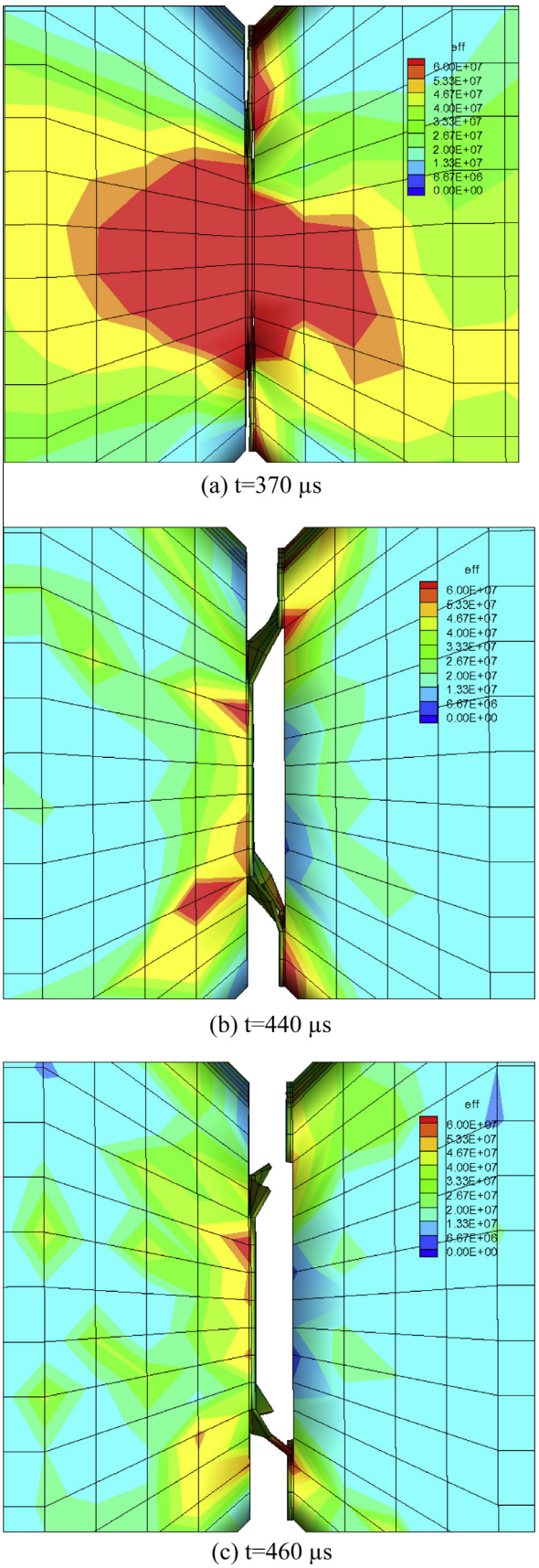

Fig. 11. Fracture process of adhesive failure of the bonded joint under tensile loading.

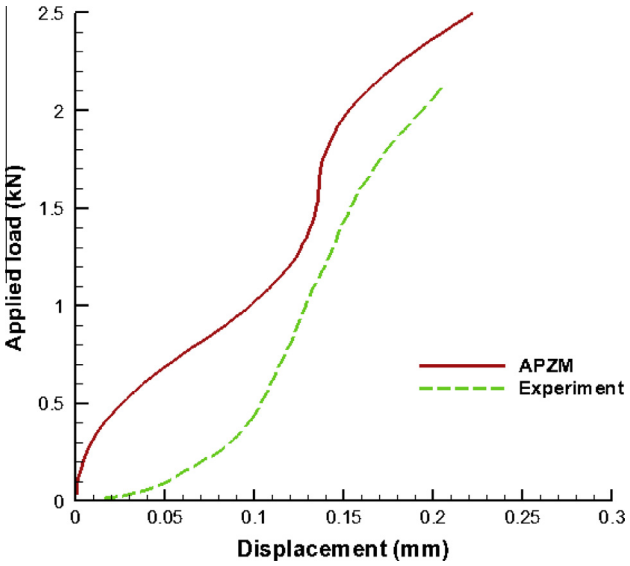

Fig. 12. Loading–deflection curves under shear–tension (mixed-mode) loading.

predict the critical strain value (0.6) that is observed in the experiment.

5. Finite element implementation

The APZM uses regular types of elements for both bulk elements and process zone elements; therefore the finite element implementation of APZM follows the standard Galerkin weak formulation discretization. Denote the computational domain in the reference configuration as Ω_0. The equation of motion in a total Lagrangian formulation may be written as follows,

$$\nabla_X \mathbf{P} + \rho_0 \mathbf{b} = \rho_0 \ddot{\mathbf{u}} \tag{11}$$

where $\mathbf{P}$ denotes the 1st Piola–Kirchhoff stress tensor, which can be related to the Cauchy stress as $\mathbf{P} = J\sigma\mathbf{F}^{-T}$; $\mathbf{b}$ denotes the body force; ρ_0 is the initial density of material, and $\mathbf{u}$ is the displacement field. Here subscripts 0 and the capital letter $\mathbf{X}$ of coordinate system refer to their association to the reference configuration.

By the weighted residual principle, the residual formulation of balance of linear momentum can be written as:

$$\int_{\Omega_0} (\nabla_X \mathbf{P} + \rho_0 \mathbf{b} - \rho_0 \ddot{\mathbf{u}}) \delta \mathbf{u} d\Omega_0 = 0 \tag{12}$$

where $\delta\mathbf{u}$ is the virtual displacement. Via integration by parts, we can derive the virtual work principle as,

$$\int_{\Omega_0} \mathbf{P} \nabla_X \delta \mathbf{u} dV - \int_{\Gamma^T} \mathbf{T} \delta \mathbf{u} dS - \int_{\Omega_0} \rho_0 \mathbf{b} \delta \mathbf{u} dV + \int_{\Omega_0} \rho_0 \ddot{\mathbf{u}} \delta \mathbf{u} dV = 0 \tag{13}$$

Here Γ^T denotes the traction boundary where the traction force $\mathbf{T}$ is prescribed.

In APZM, the stress $\mathbf{P}$ of bulk elements can be calculated based on the constitutive model of continuum mechanics, meanwhile the stress $\mathbf{P}$ of the process zone elements is calculated by using Eq. (5).

6. Simulations of bonded joint with mixture failure modes

The failure modes of bonded joints are different under shear, tension or mixed loads such as the shear–compression load. In

this work, all three types of loading conditions are used in the simulation, and the corresponding numerical results are compared with experimental data to validate the proposed APZM. According to the experimental set-up, the dimension of numerical specimen is shown as Fig. 5. The computation boundary condition for mixed mode loading is shown as Fig. 6(a).

In Fig. 6(a), the specimen orientation is horizontal. The applied load p is applied to the two areas of the specimen (10 mm length each) with a specific and the opposite direction,

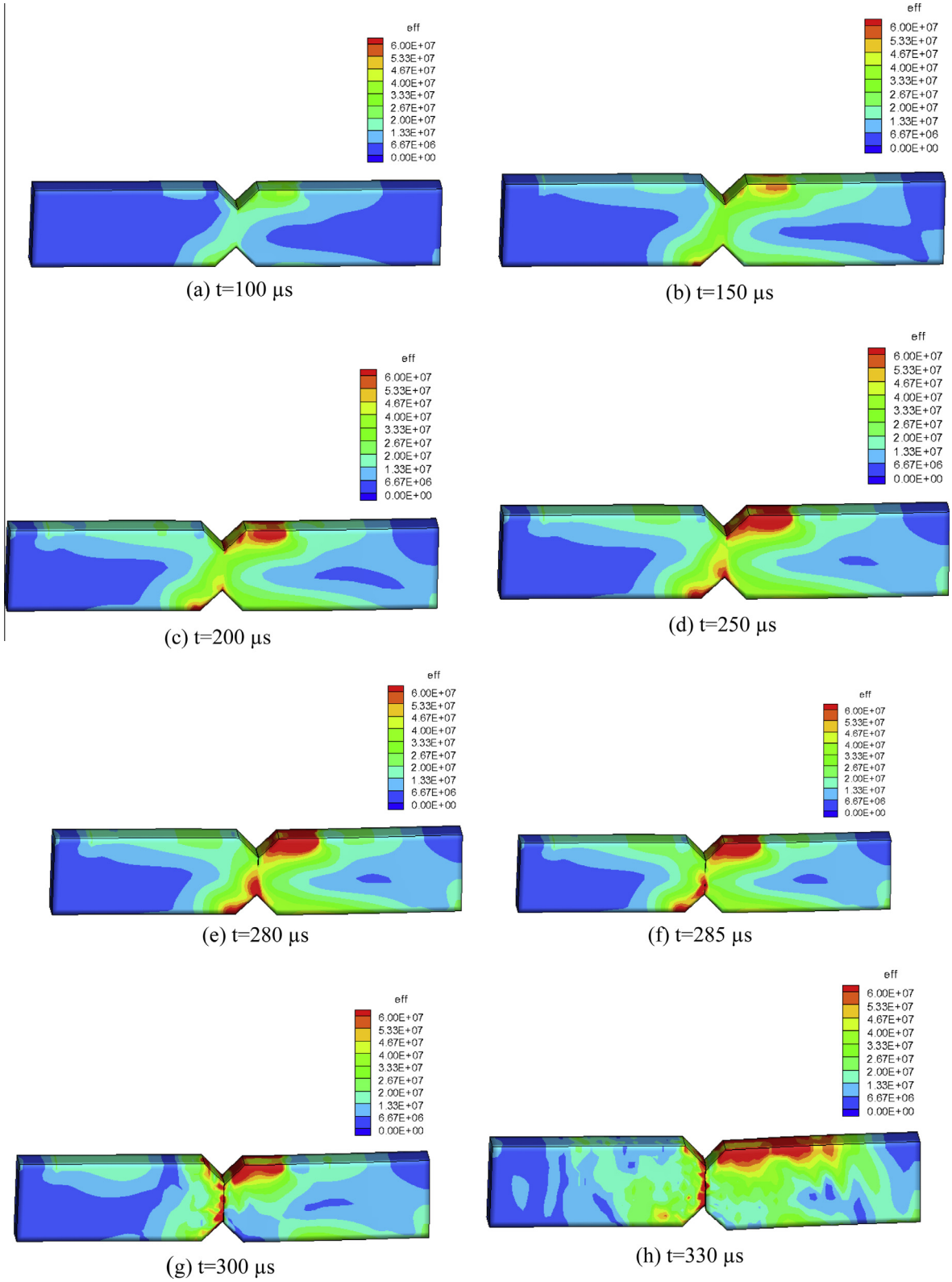

Fig. 13. The time sequences of failure process under shear–compression loading (effective stress).

which will minimize moment on the bond line. There is a loading angle α, which induces a normal ($p\cos(\alpha)$) and a shear ($p\sin(\alpha)$) load to create either a pure shear load ($\alpha = 0$) or a mixed mode load ($\alpha \neq 0$). To create a pure tensile load, we just fix one end of specimen and impose tension force p at another end. The adherend material is an Aluminum, which may be modeled as an elasto-plastic material, and the adhesive material is FM73 epoxy adhesive, whose constitutive model has been discussed in Section 4. The FEM mesh consists of 7872 nodes and 6075 brick elements. The detailed FEM meshes for the structure as well as for the bonded joint zone are shown as Fig. 8(b). The computation time step is 2.0e−8 s. The simulations are carried out in a Dell Vostro 1440 lap-top computer, and the computational time for each run ranges from 15 min to 25 min. One may find that the computational efficiency is high. The loading conditions, computational results, and experimental results are all listed in Table 2.

In this work, the onset failure load is defined as the strength of the structure, and we find that our numerical results of the structure strength can fit the experimental data very well. Fig. 3 shows that the AZPM shear stress–strain relation based on the selected adhesive potential can fit well with the shear stress–strain relation observed in experiments; subsequently the failure load obtained in the numerical simulation can fit with experiment data exactly for the case under pure shear load. Since we adjust the open parameters in the adhesive potential energy to fit the only tension constitutive relation of adhesive FM73U, therefore under the shear–tension mixed type loading or the pure tension loading, the critical failure load values are little higher than the experimental values. Under the combined shear and compression loading, there is strong effect of second contact after failure in experimental test. This effect is neglected in the simulation. Consequently the APZM critical failure load values are lower than that of experimental values. This error can be corrected, if a contact algorithm or an internal force smoothing algorithm is implemented. The details of the numerical simulations and their comparisons with experimental data are discussed in the following sections.

6.1. Simulation of pure shear load with cohesive failure mode

The time sequences of the bonded joint failure process under the pure shear loading are shown in Fig. 7.

Under the pure shear loading, the bonded joint will break in a cohesive failure mode, i.e. the fracture occurs along the interphase elements. The detailed cohesive failure process is shown in Fig. 8. It should be noted that during the shearing test, the specimen actually fractures at the bottom first.

The comparison of load–deflection curves between the experimental results and the APZM simulation results is shown in Fig. 9. Here we would like to point out that the experimental data is obtained under a quasi-static loading condition, whereas the numerical result is obtained in a dynamic process. Therefore the shape of the load–deflection curves of APZM prediction is slightly different from that of the experimental result. Furthermore, all the experimental curves in Figs. 9, 12 and 15 have a smaller slope segment at beginning because of the initial slip during the tests. This initial slips result in a larger critical deflection (displacement) than the actual displacement. However, the critical load, on the hand, is close to the actual critical load. To neglect the influence of initial slip, the comparable characteristics of numerical and experimental results are the critical loads, the slops of the main segments of numerical and experimental curves as well as the failure modes. One can find that these characteristics are compared well between the numerical simulation results and the experimental data.

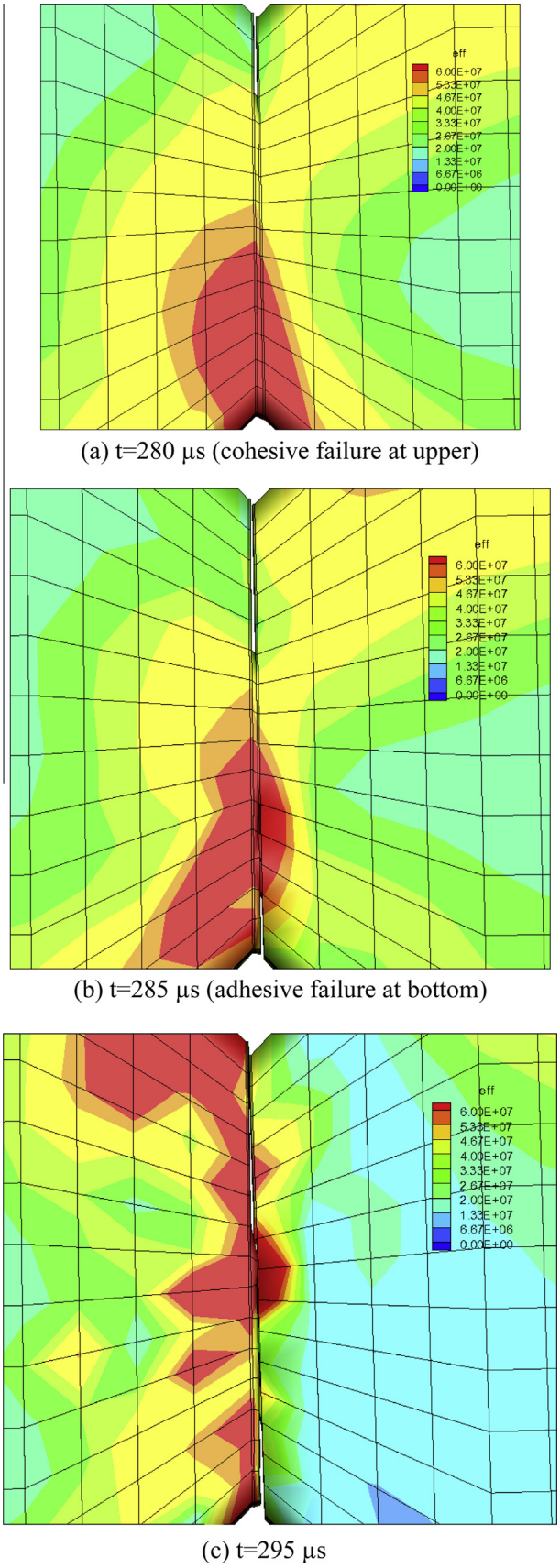

(a) t=280 μs (cohesive failure at upper)

(b) t=285 μs (adhesive failure at bottom)

(c) t=295 μs

Fig. 14. Dynamic process of adhesive–cohesive failure.

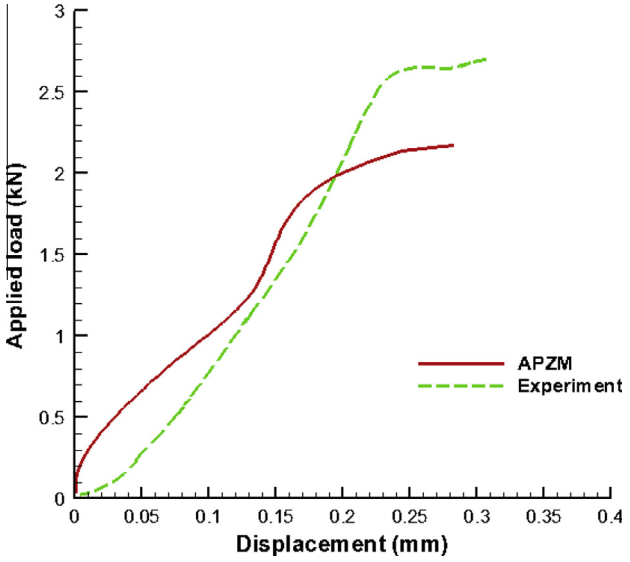

Fig. 15. Loading–deflection curves under combined shear–compression loading.

6.2. Simulation of pure tension loading with adhesive failure mode

From APZM simulations, we have found that the tension loading under dynamic condition will result adhesive failure mode. To elucidate this process, we have recorded the time sequences of the bonded joint failure process under tension loading, which are shown in Fig. 10.

From Fig. 10, one can clearly observe that under the tensile loading, the bonded joint will break in an adhesive failure mode, i.e. the crack path is along transit elements. To observe the detailed fracture morphology, we show a zoom-in slow fracture process in Fig. 11.

The comparison of the loading–deflection curves between experimental results and numerical result are also displayed in Fig. 12.

6.3. Simulation of the mixture mode failure under mixed-mode loading

In this subsection, we present the simulation results obtained under the combined shear–compression loading, which results a mixture mode failure for the bonded joint. We first show the time sequences of the bonded joint failure process under the shear–compression loading in Fig. 13.

Under the combined shear–compression loading, the bonded joint will break in a mixture failure mode, i.e. a concurrent cohesive failure and adhesive failure, in which the crack occurs in both transit elements as well as interphase elements. The detailed failure process is shown in Fig. 14.

The loading–deflection curves of the experimental data and the numerical result are compared in Fig. 15.

7. Conclusions

In this paper, we present the theoretical and numerical analysis of a multiscale APZM model for the bonded joints. It is shown that the proposed model is capable of simulating the dynamic responses of the bonded joint structures, and it can capture the complicated failure modes under complex loading conditions. The APMZ is a novel and advantageous method that, we believe, may change the engineering analysis of the bonded joint structures.

Referring to the geometric configurations and physical failure morphologies of the bonded joints, APZM combines the advantages of CZM and VIB theory, i.e., it not only can capture material fracture process automatically as CZM, but also predict complex fracture patterns under mixed-mode loadings. This is due to the VIB theory's ability to access all components of stress state inside the process zone instead of using the ad-hoc traction–separation laws as CZM. Therefore, APZM prediction is more accurate than that of CZM calculation. We have found in the simulation that the relative motions of adjacent adherends due to the "glue" of adhesive is dictated by the complex 3D stress fields, and they cannot be predicted by using CZM type of interface model because of the inadequacy and inaccuracy of the stress field evaluation.

In particular, we have discovered in the simulation that: (1) the pure shear loading may result in an adhesive failure mode; (2) the pure tensile loading may result in a cohesive failure, and (3) the combined shear–compression mixed mode loading may result a mixture failure mode. Hence, it is fair to say that APZM can predict realistic joint failure modes such as cohesive failure, adhesive failure, and adhesive–cohesive mixture failure mode naturally. In comparison with the CZM, APZM integrates both of adherends and adhesive process zone in a single framework of multiscale FEM formulation, and it makes it easy to be implemented and integrated with commercial FEM software.

The present work models the adherends by using conventional FEM technology; it works well for the most homogeneous adherend materials. However, the past experimental and engineering experiences have revealed that the failure may occur in the composite adherends, which is called as first-ply-failure, or the cracks may reach the adherends through adhesive. For these cases, specific layers of adherends must be treated by APZM as well, or one has to employ X-FEM in simulation of adherends.

References

[1] P.E. Lyon, Axisymmetric Finite Element Modeling for the Design and Analysis of Cylindrical Adhesive Joints Based on Dimensional Stability, Master Thesis, Mechanical Engineering, Utah State University, U.S.A., 2010.
[2] O. Volkersen, Rivet strength distribution in tensile-stressed rivet joints with constant cross section, Luftfehrforschung 15 (1938) 41–47.
[3] M. Goland, E. Reissner, The stresses in cemented joints, J. Appl. Mech. Trans., ASME 66 (1944) A17–A27.
[4] A.D. Crocombe, D.A. Bigwood, Elastic analysis and engineering design formulae for bonded joints, Int. J. Adhes. Adhes. 9 (1989) 229–242.
[5] Y. Zhu, K. Kedward, Methods of analysis and failure predictions for adhesively bonded joints of uniform and variable bondline thickness, in: Report No. DOT/FAA/AR-05/12, 2005.
[6] A. Kaya, Three dimensional stress analysis in adhesively bonded joint, Math. Comput. Appl. 3 (2) (1998) 101–111.
[7] M. Zgoul, Characterising the Rate Dependent Response of Adhesively Bonded Structures, Ph.D Thesis, School of Engineering, University of Surrey Guildford, U.K., 2002.
[8] J.S. Bergström, M.C. Boyce, Deformation of elastomeric networks: relation between molecular level deformation and classical statistical mechanics models of rubber elasticity, Macromolecules 34 (2001) 614–626.
[9] J.S. Tomblin, C. Yang, P. Harter, Investigation of thick bondline adhesive joints, in: Report No. DOT/FAA/AR-01/33, 2001.
[10] L.J. Hart-Smith, Adhesive Bonded Single Lap Joints, NASA CR12235, 1973.
[11] M.M. Ratwani, H.P. Kan, D.D. Liu, Time-dependent adhesive behavior effects in a stepped-lap joint, AIAA J. 20 (5) (1982) 734–736.
[12] M. Ignjatovic, P. Chalkley, C. Wang, Yield behavior of a structural adhesive under complex loading, in: Airframes and Engines Division, Aeronautical and Maritime Research Laboratory, Report No. DSTO-TR-0728, 1998.
[13] M.C. Song, B.V. Sankar, G. Subhash, C.F. Yen, Analysis of mode I delamination of z-pinned composites using a non-dimensional analytical model, Composites Part B 43 (2012) 1776–1784.
[14] R.D.S.G. Campilho, M.F.S.F. de Moura, J.J.M.S. Domingues, Using a cohesive damage model to predict the tensile behavior of CFRP single-strap repairs, Int. J. Solids Struct. 45 (5) (2008) 1497–1512.
[15] B. Ren, S.F. Li, A three-dimensional atomistic-based process zone model simulation of fragmentation in polycrystalline solids, Int. J. Numer. Meth. Eng. 93 (2013) 989–1014.
[16] H. Gao, B. Ji, Modeling fracture in nanomaterials via a virtual internal bond method, Eng. Fract. Mech. 70 (2003) 1777–1791.
[17] E.W. Thrall, Primary adhesively bonded structure technology (PABST), J. Aircraft 14 (6) (1977) 588–594.

[18] J. Tomblin, W. Seneviratne, P. Escobar, Y. Yoon-Khian, Shear Stress–Strain Data for Structural Adhesives, in: Report No. DOT/FAA/AR-02/97, 2002.
[19] X. Zeng, S. Li, A multiscale cohesive zone model and simulations of fractures, Comput. Methods Appl. Mech. Eng. 199 (2010) 547–556.
[20] S. Li, X. Zeng, B. Ren, J. Qian, J. Zhang, A.J. Jha, An atomistic-based interphase zone model for crystalline solids, Comput. Methods Appl. Mech. Eng. 229–232 (2012) 87–109.
[21] X. Zhuang, C. Augarde, K. Mathisen, Fracture modelling using meshless methods and level sets in 3D: framework and modelling, Int. J. Numer. Meth. Eng. 92 (2012) 969–998.
[22] P.R. Budarapu, R. Gracie, S.W. Yang, X. Zhuang, T. Rabczuk, Efficient coarse graining in multiscale modeling of fracture, Theoret. Appl. Fract. Mech. 69 (2014) 126–143.
[23] N. Vu-Bac, T. Lahmer, Y. Zhang, X. Zhuang, T. Rabczuk, Stochastic predictions of interfacial characteristic of polymeric nanocomposites (PNCs), Composites Part B 59 (2014) 80–95.
[24] E.M. Arruda, M.C. Boyce, A three-dimensional constitutive model for the large stretch behavior of rubber elastic materials, J. Mech. Phys. Solids 41 (1993) 389–412.